韓國環境衛生學會誌
Kor. J. Env. Hlth. Soc.
Vol. 17, No. 1, 39~49, 1991

# Development of Porous Sorbents for Removal of Hydrogen Sulfide from Hot Coal Gases

## Ⅲ. Study on Ferrite-type adsorbent for the Removal of Hydrogen Sulfide

Jong Saeng Kim · Young Soo Lee · Jae Bok Lee* · Kyong Ok Yoo

*Dept. of Chemical Engineering Hanyang University*
**Dept. of Chemical Engineering Samcheok Industrial Univ.*

## 要 旨

고온에서 황화수소($H_2S$)를 제거하기 위한 흡착제를 개발할 목적으로 ZnO에 $Fe_2O_3$를 5~50 atomic %까지 첨가시켜 제조한 다공성 흡착제와 황화수소와의 반응(sulfidation)을 thermogravimetric analyzer (shimadzu DT-30)로 수행하였으며, 고정층에서 zinc ferrite 흡착제의 흡착능을 측정하였다.

반응온도는 723°K~973°K범위이며, 반응기체는 황화수소(2vol. %)와 질소와 혼합기체로서 total gas flow rate는 200ml/min으로 고정시켰다.

Grain Model을 사용하여 실험데이터를 분석한 결과 전화율이 낮을 때 zinc ferrite와 황화수소 반응의 율속단계는 화학반응이었고 황화수소 농도에 대해 1차 반응이었다. 실험한 흡착제 중 10 atomic %의 $Fe_2O_3$를 첨가하여 제조한 zinc ferrite형 흡착제가 반응속도, 흡착능, 그리고 재생성면에서 우수한 흡착제로 밝혀졌다.

## Ⅰ. Introduction

Coal gasification process to produce fuel has been developed for many years. The major deteriorating factor of this process is the contaminants like $SO_2$, $NO_2$, $H_2S$ in the product gas stream. Especially, control of hydrogen sulfide ($H_2S$) gas which is very toxic and corrosive to a safe level is essential. Although conventional process called cold scrubbing technique[1,2] is effective for removal of $H_2S$, it has drawbacks due to loss of sensible heat of the gas.

Recently it has been reported that metal oxide or mixed metal oxide sorbents enhance the effiency of $H_2S$ removel in hot coal-derived gas[3]. Westmoreland et al.[4] reported studies on the reaction of $H_2S$ with metal oxides such as MnO, CaO, ZnO, and $V_2O_3$. They suggested that all reations be the first order with respect to gas concentration.

Anderson et al.[5] reported zinc aluminate and zinc chlomite were appropriate for the des-

ulfurization and regeneration of produced sulfate. For actual industry, these sorbents will reduce 50% of operating cost and 70% of energy desired compared to those of acid gas removal at low temperature or Clauss process.

Won and Sohn[6] analyzed the reaction of $H_2S$ gas with dolomite with pore blocking model. Krimshan et al.[7] calculated thermodynamic equilibrium and explained the procedure of sulfate formation through the regeneration of ZnO, $Fe_2O_3$ and $ZnFe_2O_4$ sorbents.

Tamhankar et al.[8] suggested iron oxide ($Fe_2O_3$ 45.wt%-$SiO_2$ 55.wt%) be the best suitable sorbent for $H_2S$ removal on the basis of adsorption efficiency, mechanical strength and regeneration. Executing the reaction of $H_2S$ with mixed metal oxides like ZnO, CuO, ZnO-$Fe_2O_3$, CuO-$Fe_2O_3$, CuO-$Al_2O_3$ and CuO-$Fe_2O_3$-$Al_2O_3$, Gevalas et al[9] reported CuO-$Fe_2O_3$, CuO-$Al_2O_3$ and CuO-$Fe_2O_3$-$Al_2O_3$ were good for desulfurization and regeneration. Grindly and Seinfield[10] nominated zinc ferrite for desulfurization of coal-derived gas. We find out that, on the ground of seqential studies of our labolatory,[11,12] porous ZnO sorbent prepared special method exhibits good efficiency of desulfurization and regeneration, however, its application to actual industry is difficult because of weak mechanical strength. In this present work, our aim is development of sorbents having similar properties of ZnO and high mechanical strength by adding the $Fe_2O_3$ to ZnO.

## Ⅱ. Experiment

### 1. Preparation of Sorbent

A. Porous, particle-type sorbents

Sorbents are prepared as follows ;

1) Mixing of two metal oxides

2) Adding of blowing agent to mixture

3) Dissolving with distillated water and agitation

4) Reserving in drying oven at 65~70℃ for 4~5 hours.

5) Reserving in vaccum oven connected by dry ice trap for 1 day.

6) Calcining at 600℃ under the flow of oxygen for 3~5 hours.

### 2. Charicterization of Sorbent.

X-ray diffraction pattern of fresh sorbent is dipicted in Fig. 1 and our major sorbent is Zinc ferrite($ZnFe_2O_4$). Fig. 2 shows the SEM photographs of zinc ferrite containing 10wt% $Fe_2O_3$. Table 1. lists the porosity and specific

Table 1. Specific surface area and prorosity of sorbents

| Sorbents | Specific surface area ($m^2/g$) | Porosity (%) |
|---|---|---|
| ZnO-10 at. % $Fe_2O_3$ | 13.88 | 50.12008 |
| *ZnO-15 at. % $Fe_2O_3$ | 10.14 | 45.13695 |
| ZnO-20 at. % $Fe_2O_3$ | 6.40 | 40.15382 |
| ZnO-25 at. % $Fe_2O_3$ | 11.61 | 45.80848 |
| ZnO-30 at. % $Fe_2O_3$ | 8.84 | 36.76268 |
| ZnO-35 at. % $Fe_2O_3$ | 17.29 | 47.34374 |
| ZnO-40 at. % $Fe_2O_3$ | 13.02 | 58.77958 |
| ZnO-45 at. % $Fe_2O_3$ | 6.73 | 48.87674 |
| ZnO-50 at. % $Fe_2O_3$ | 9.37 | 64.25113 |

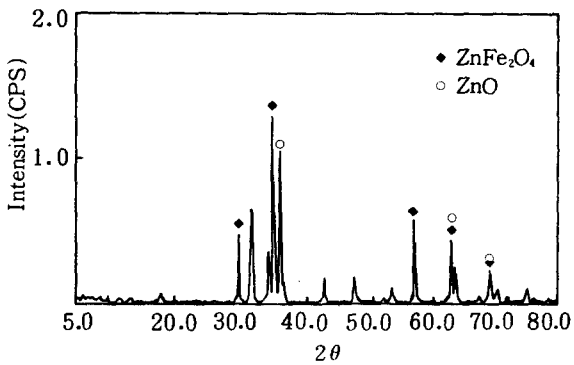


Fig. 1. XRD pattern of the sorbent (ZnO-10 at. % $Fe_2O_3$)


Fig. 2. Scanning electron micrograph of porous ZnO-10 at. % $Fe_2O_3$.

surface area of various sorbents obtained from porosimetry. Porosity and specific surface area is 36~65% and 6~18$m^2$/g, respectively.

### 3. Apparatus and Procedure

The schematic diagram of the experimental set-up is depicted in Fig. 1 Experimental set-up is devided into two parts, namely, TGA (shimadzu DT-30) and controlling section of flow rate. The reacting and dilute gases from regulated cylinders passed through purifiers and then through calibrated soap flow meter connected by needle valve to a common gas line. The sorbents reserved in vaccum decicator before experiments were particle type (20~30 mesh) and pellet type (0.3cm d. ×0.316cm length). When the constancy of the reaction temperature is checked, reacting gas were introduced into TGA. The weight gain of the sample versus time is recoreded continously by recorder. Completion of the reaction was conformed by the constancy of the sample weight for a long time. After completion of reaction, purging with nitrogen gas is executed to prevent the oxidation of produced surfate and corrosion of apparatus. The effect of total gas flow rate on reaction rate is shown in Fig. 4 This shows that the flow rate has no effect on

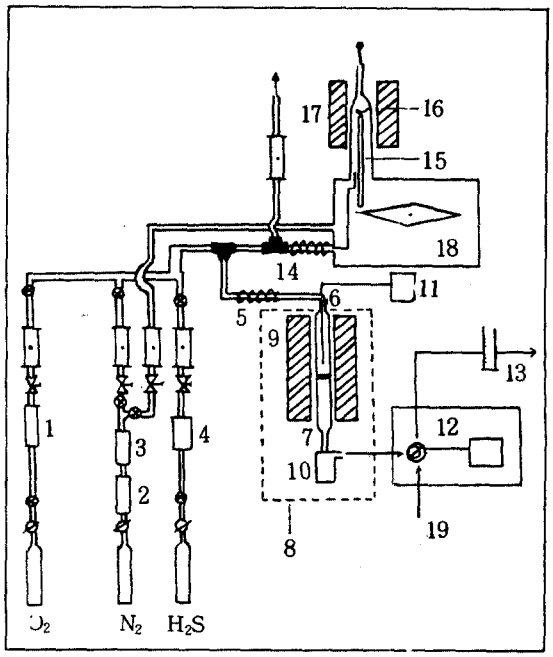


Fig. 3. Schematic digram of experimental apparatus.

1. Zeolite trap
2. Zeolite trap
3. Purifier
4. Silicagal trap
5. Preheater
6. Thermocouple
7. Quartz reactor
8. Fixed bed
9. Furnace
10. Sulfur trap
11. Temperature controller
12. G. C
13. Soap flowmeter
14. Three-way valve
15. Detector
16. Sample cell
17. Furnace
18. T.G.A.
19. Carrier gas

the reaction rate, that is, there is no resistance to gas film diffusion above 200ml/min. Other experimental conditions are listed in Table 2.

Table 2. Experimental condition of reaction

| |
|---|
| Reaction temperature : 723~973K |
| Gas composition : $H_2S$ 2 vol % |
| $N_2$ 98 vol % |
| Sorbents ($ZnFe_2O_4$) : particle type 20~30mesh |
| $Fe_2O_3$ content of sorbent : 5~50 atomic % |
| Total gas flow rate : 200ml/min |
| Total pressure : 1.0atm |

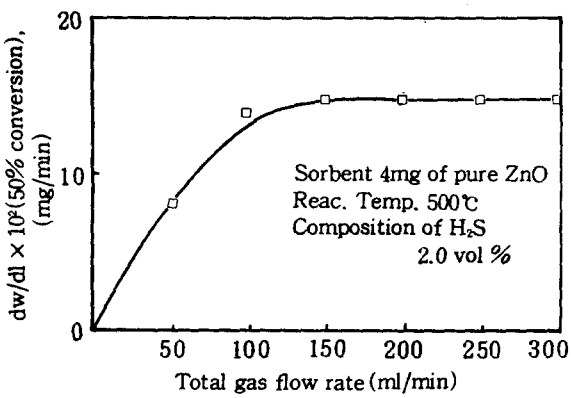


Fig. 4. Effect of total gas flow rate on the reaction rate.

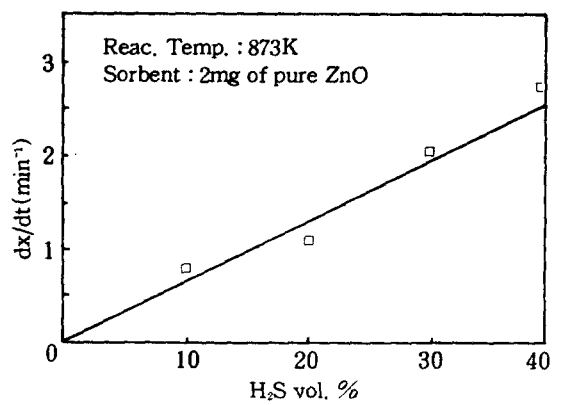


Fig. 5. Dependence of $H_2S$-concentration on the reaction rate.

### 4. Experiment for Adsorption Efficiency

To obtain the adsorption efficiency, quartz tube (2.5cm o.d×1m length) packed with zinc

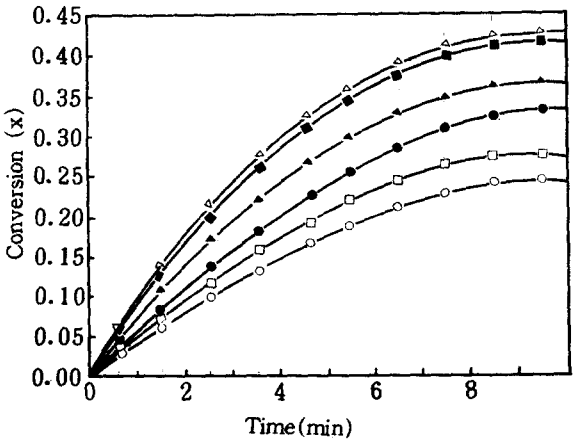


Fig. 6. Conversion-time curve for the sorbents at 723°K.

- ■ ZnO-10 at. % $Fe_2O_3$
- □ ZnO-40 at. % $Fe_2O_3$
- ▲ ZnO-20 at. % $Fe_2O_3$
- ○ ZnO-50 at. % $Fe_2O_3$
- ● ZnO-30 at. % $Fe_2O_3$
- △ Pure ZnO

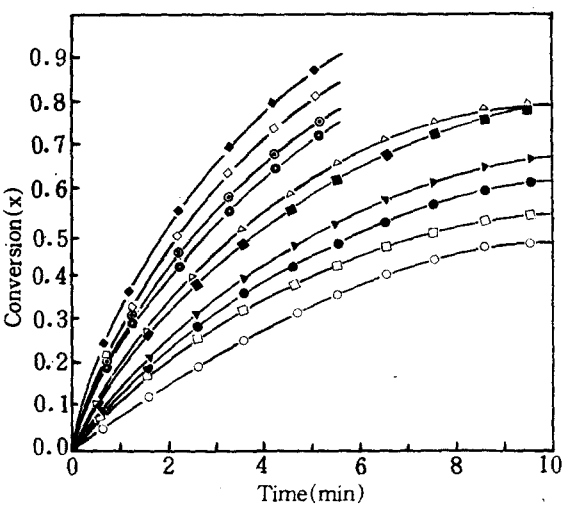


Fig. 7. Conversion-time curve for the sorbents at 773°K.

- ◆ ZnO-2.0 at. % $Fe_2O_3$
- ▲ ZnO-20 at. % $Fe_2O_3$
- ◇ ZnO-1.5 at. % $Fe_2O_3$
- ● ZnO-30 at. % $Fe_2O_3$
- ◉ ZnO-1.0 at. % $Fe_2O_3$
- □ ZnO-40 at. % $Fe_2O_3$
- ● ZnO-0.5 at. % $Fe_2O_3$
- ○ ZnO-50 at. % $Fe_2O_3$
- ■ ZnO-10 at. % $Fe_2O_3$
- △ Pure ZnO

ferrite(ZnO-10 at.% $Fe_2O_3$) 100g was used under the conditions described at Table 2, at 700℃. The space velocity of this case is 244 $hr^{-1}$.

Produced gases were condensed to elemental sulfur in ice-trap and $H_2S$ and SOx in the produced gases were analyzed by G.C.

After sulfidation of ZnO, $N_2$ passed through the packed bed for 30 minutes to purge the $H_2S$ gas completely and redox experiments($O_2$ regeneration+$H_2S$ sulfidation) were carried out at 700℃.

## Ⅲ. Expermental Results and Discussion.

The stiochimetric equation of zinc ferrite with $H_2S$ is

$$ZnFe_2O_4(s) + 3H_2S(g) = ZnS(s) + 2FeS(s) + 3H_2O(g) + 1/2O_2(g) \quad \cdots\cdots(1)$$

and the conversion is

$$X = \frac{W_o - W}{W_o(1 - M/Ms)} \quad \cdots\cdots(2)$$

Where Wo is initial weight of sorbent
W is weight of sorbent at arbitary time t,
M is molecular weight of $ZnFe_2O_4$
Ms is molecular weight of sulfate like ZnS and FeS.

The results of sulfidation of zinc ferrite obtained from above method is shown as follows ;

### 1. Effect of $H_2S$ concentration on reaction rate

The relationship between the initial reation rate (dx/dt) and $H_2S$ concentration is depicted in Fig. 5. We found out that sulfidation rate of zinc ferrite was the first order with respect to the $H_2S$ concentration.

### 2. Additive effect of porous particle type sorbent

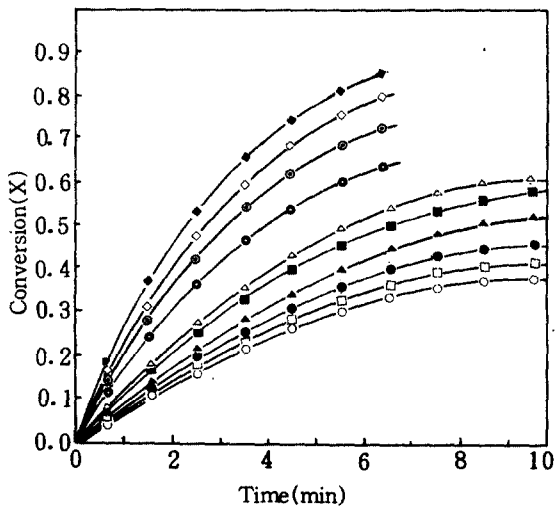


Fig. 8. Conversion-time curve for the sorbents at 873°K.

- ◆ ZnO-2.0 at. % $Fe_2O_3$
- ◇ ZnO-1.5 at. % $Fe_2O_3$
- ◉ ZnO-1.0 at. % $Fe_2O_3$
- ● ZnO-0.5 at. % $Fe_2O_3$
- ■ ZnO-10 at. % $Fe_2O_3$
- ▲ ZnO-20 at. % $Fe_2O_3$
- ● ZnO-30 at. % $Fe_2O_3$
- □ ZnO-40 at. % $Fe_2O_3$
- ○ ZnO-50 at. % $Fe_2O_3$
- △ Pure ZnO

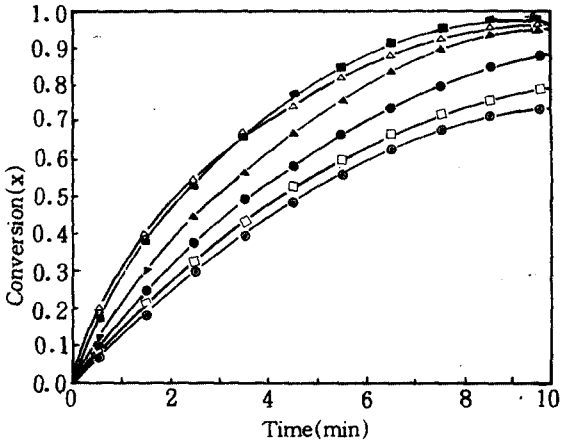


Fig. 9. Conversion-time curve for the sorbents at 973°K.

- ■ ZnO-10 at. % $Fe_2O_3$
- ▲ ZnO-20 at. % $Fe_2O_3$
- ● ZnO-30 at. % $Fe_2O_3$
- □ ZnO-40 at. % $Fe_2O_3$
- ● ZnO-50 at. % $Fe_2O_3$
- △ Pure ZnO

The conversion-time curves for ZnO 5~50 at.% $Fe_2O_3$ sorbent at 723, 773, 873, and 973 K are shown in Fig. 6 ~ Fig. 9.

Fig. 7 and Fig. 8 obtained from reference (13) are compared with our data. Fig. 6 shows ZnO goes beyond the ZnO-10~15 at.% $Fe_2O_3$ sorbents and ZnO-10 at % $Fe_2O_3$ sorbent has a similar conversion with ZnO. $Fe_2O_3$ amount is the more, conversion is the less. Fig. 7 shows zinc ferrite containing 0.5~2.0 at% $Fe_2O_3$ has high conversion than that of ZnO and the conversion is decreased when additive amount of $Fe_2O_3$ is above 10 at%. Fig. 8 has similar features of Fig. 7. Zinc ferrite containing 10~50 at. % $Fe_2O_3$ has lower conversion than that of ZnO. When additive amount of $Fe_2O_3$ is above 10 at.%, $Fe_2O_3$ amount is the more, conversion is the less. From the Fig. 9, we find out that Zinc ferrite containing 20~50 at% $Fe_2O_3$ has lower conversion than that of ZnO before 3 minues, the reverse feature appears after 3 minutes.

This phenomenon is considered to be caused the vaporization of ZnO. From the above informations, zinc ferrite containing 2.0 at.% $Fe_2O_3$ is the best, however, the mechanical strength is weak like ZnO. To enhance the reaction rate and mechanical strenght, $Fe_2O_3$ is added to ZnO. We conclude the reaction rate of zinc ferrite containing 10 at.% $Fe_2O_3$ is similar with ZnO and mechanical strength is enhanced.

### 3. Reaction Mechanism of particle type Sorbent with $H_2S$

For gas-solid reaction

$$A(g) + bB(s) = cC(g) + dD(s) \quad \cdots\cdots (3)$$

of which controlling step is chemical reaction, the material balance of reactant A and B based on the unit surface area of solid reactant B is

$$\frac{1}{b \cdot 4\pi r^2} \frac{dN_B}{dt} = \frac{1}{4\pi r^2} \frac{dN_A}{dt} = K_S C_{AO} \quad (4)$$

where,

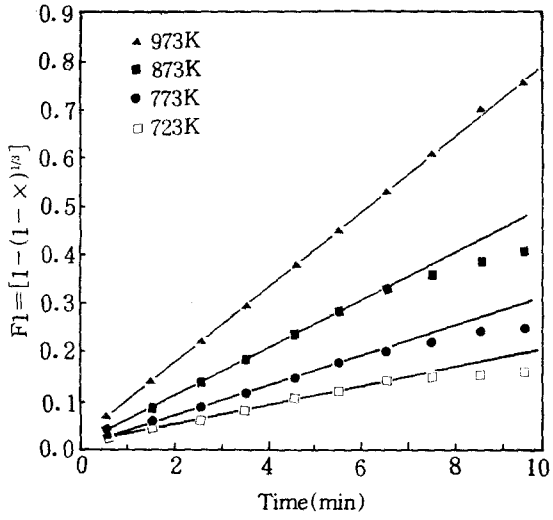


Fig. 10. Conversion function-time for the sorbents (ZnO-10 at. % $Fe_2O_3$).

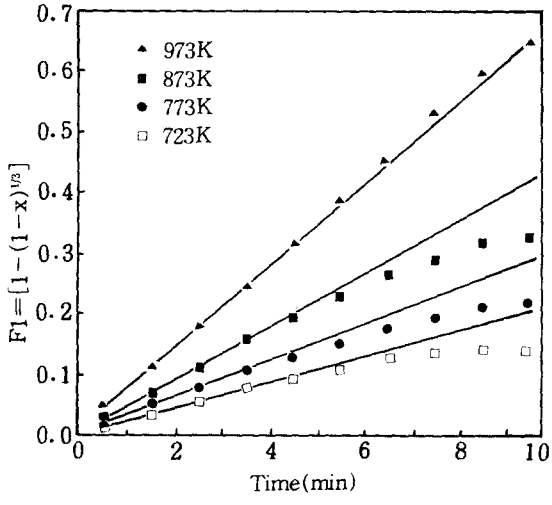


Fig. 11. Conversion function-time for the sorbents (ZnO-20 at. % $Fe_2O_3$).

$$dN_B = d[\rho V(1-\varepsilon)/M] \quad \cdots\cdots (5)$$

If the solid reactant B is spherical ($V = 4/3\pi r^3$), Eg(5) is rewritten as

$$dN_B = \frac{4\pi r^2 \rho(1-\varepsilon)}{M} \quad \cdots\cdots (6)$$

substituting Eg. (6) to Eg(4) We obtain

$$-\frac{\rho(1-\varepsilon)}{M}\,dr = b\cdot k_s\cdot C_{AO}\cdot dt \quad \cdots\cdots\cdots\cdots (7)$$

As the diameter is changed from R to r according to the change of reaction time from O to t, Integration of Eg(7) is

$$\frac{\rho(1-\varepsilon)}{M}\,[1-(r/R)] = b\cdot k_s\cdot C_{AO}\cdot t \quad \cdots\cdots\cdots (8)$$

Fractional conversion is

$$X = 1-(r/R)^3 \text{ or } (r/R) = (1-X)^{1/3} \quad \cdots\cdots\cdots (9)$$

And substitution of eq. (8) becomes

$$t = \frac{\rho(1-\varepsilon)R}{b\cdot k_s\cdot C_{AO}\cdot M}\,[1-(1-X)^{1/3}] \quad \cdots\cdots\cdots\cdots (10)$$

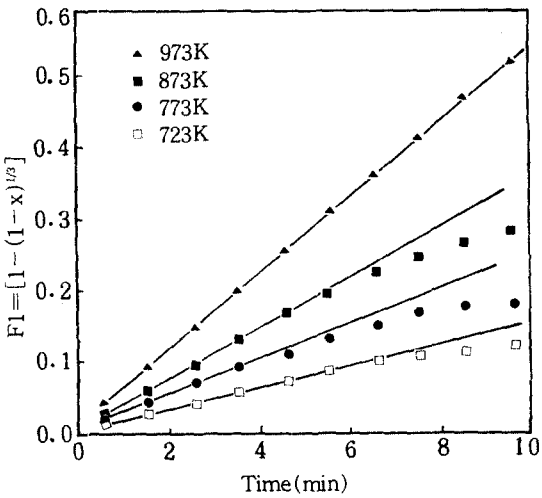


Fig. 12. Conversion function-time for the sorbents (ZnO-30 at. % $Fe_2O_3$).

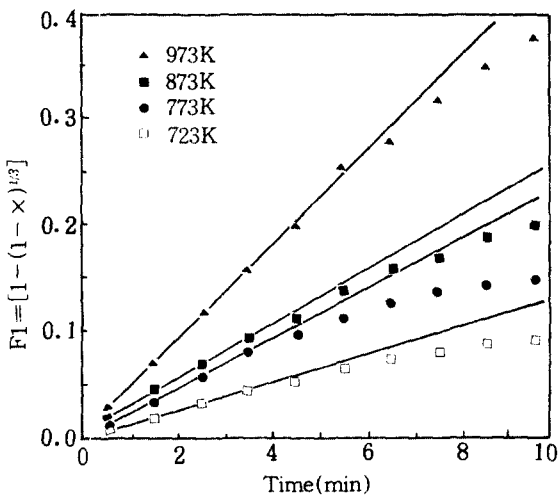


Fig. 14. Conversion function-time for the sorbents (ZnO-50 at. % $Fe_2O_3$).

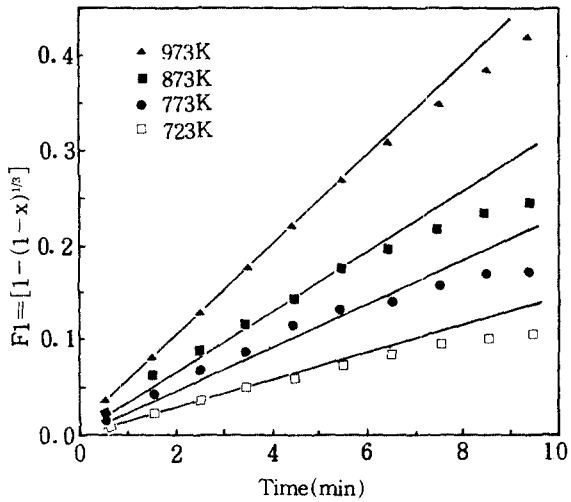


Fig. 13. Conversion function-time for the sorbents (ZnO-40 at. % $Fe_2O_3$).

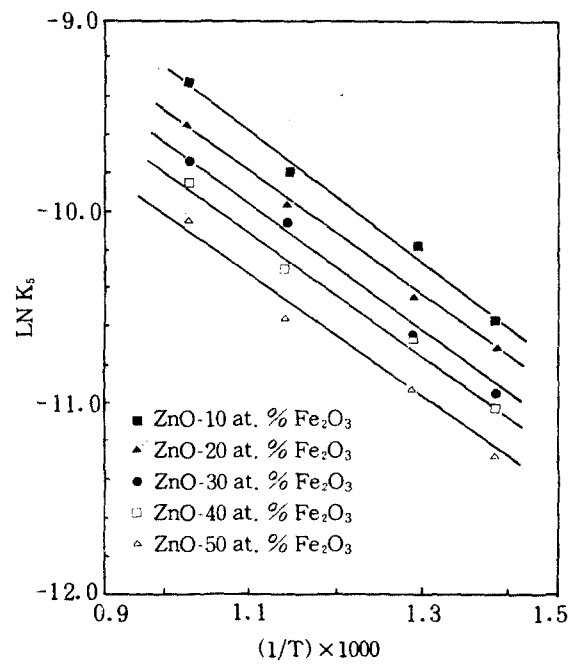


Fig. 15. Arrhenius plot of the particle-type zinc ferrite.

Table 3. Time parameter

| Temperature / Sorbents | Time parameter ($t_1$) | | | |
|---|---|---|---|---|
| | 723K | 773K | 873K | 973K |
| ZnO-0.50 at. % $Fe_2O_3$ | | 17.38632 | 6.662010 | |
| ZnO-1.00 at. % $Fe_2O_3$ | | 15.93474 | 6.159400 | |
| ZnO-1.50 at. % $Fe_2O_3$ | | 15.27740 | 5.967436 | |
| ZnO-2.00 at. % $Fe_2O_3$ | | 14.90577 | 5.704815 | |
| ZnO-5.00 at. % $Fe_2O_3$ | 61.91359 | 32.28048 | 19.61313 | 11.94715 |
| ZnO-10.0 at. % $Fe_2O_3$ | 48.61521 | 28.81645 | 17.98556 | 9.974774 |
| ZnO-15.0 at. % $Fe_2O_3$ | 61.16844 | 30.95447 | 18.49012 | 11.84889 |
| ZnO-20.0 at. % $Fe_2O_3$ | 65.24943 | 33.90984 | 21.96762 | 13.90393 |
| ZnO-25.0 at. % $Fe_2O_3$ | 68.48925 | 37.24599 | 23.60764 | 15.28823 |
| ZnO-30.0 at. % $Fe_2O_3$ | 73.52729 | 40.07925 | 25.93119 | 16.75895 |
| ZnO-35.0 at. % $Fe_2O_3$ | 80.31645 | 42.82665 | 27.99016 | 17.69880 |
| ZnO-40.0 at. % $Fe_2O_3$ | 87.83175 | 47.49946 | 31.77499 | 19.57154 |
| ZnO-45.0 at. % $Fe_2O_3$ | 94.40150 | 53.01422 | 34.53178 | 20.40209 |
| ZnO-50.0 at. % $Fe_2O_3$ | 102.1708 | 62.95609 | 41.45440 | 21.01277 |

Table 4. Reaction rate constant and activation energy

| Temperature / Sorbents | $k_s \times 10^{-5}$(cm/sec) | | | | *Ea* |
|---|---|---|---|---|---|
| | 723K | 773K | 873K | 973K | cal/gmol |
| ZnO-5.00 at. % $Fe_2O_3$ | 2.267 | 3.003 | 6.002 | 8.726 | 7,791.881 |
| ZnO-10.0 at. % $Fe_2O_3$ | 2.756 | 4.219 | 6.794 | 11.540 | 7,765.931 |
| ZnO-15.0 at. % $Fe_2O_3$ | 2.067 | 3.928 | 6.509 | 8.721 | 7,773.065 |
| ZnO-20.0 at. % $Fe_2O_3$ | 1.863 | 3.585 | 5.453 | 8.195 | 7,820.812 |
| ZnO-25.0 at. % $Fe_2O_3$ | 1.775 | 3.264 | 5.510 | 7.690 | 7,828.462 |
| ZnO-30.0 at. % $Fe_2O_3$ | 1.653 | 3.033 | 4.688 | 7.254 | 7,855.823 |
| ZnO-35.0 at. % $Fe_2O_3$ | 1.514 | 2.839 | 4.349 | 6.725 | 7,889.324 |
| ZnO-40.0 at. % $Fe_2O_3$ | 1.384 | 2.560 | 3.826 | 6.212 | 7,903.829 |
| ZnO-45.0 at. % $Fe_2O_3$ | 1.288 | 2.289 | 3.521 | 5.959 | 8,210.273 |
| ZnO-50.0 at. % $Fe_2O_3$ | 1.190 | 1.931 | 2.933 | 5.786 | 8,377.331 |

Putting $F_1 = 1-(1-X)^{1/3}$ (11) and

$$t_1 = \frac{\rho(1-\varepsilon)R}{b \cdot C_{A0} \cdot M \cdot K_s} \quad \cdots\cdots (12)$$

Eq(10) becoems $F_1 = t/t_1$ ····· (13)

Eq.(13) means that we can find out chemical reaction rate constant $k_s$ and predict the conversion from time parameters $t_1$ obtained from conversion function-time data.

The reactions between $F_1$ and t for zinc ferrite sorbents containing 10, 20, 30, 40, and 50 at% $Fe_2O_3$ at various temperatures are depicted in Fig. 10~Fig. 14 with the aids of Fig. 6~Fig. 9 data.

As all the relations between $F_1$ and t are linear, we obtained the time parameter $t_1$ from the slope and listed in Table 3. The $t_1$ values of sorbents containing 5, 15, 25, 35 and 45 at.% $Fe_2O_3$ are also listed in Table 3. The reaction

rate constants $k_s$ gained from the $t_1$ values of Table 3 are listed in Table 4. Fig. 15 shows Arrehenius plot of rate constants of Table 4, which is somewhat linear. The dependence of rate constant on temperature (723~923 K) for each sorbent is as follows :

for ZnO−10 at.% $Fe_2O_3$ $k_s = 0.00628\exp$

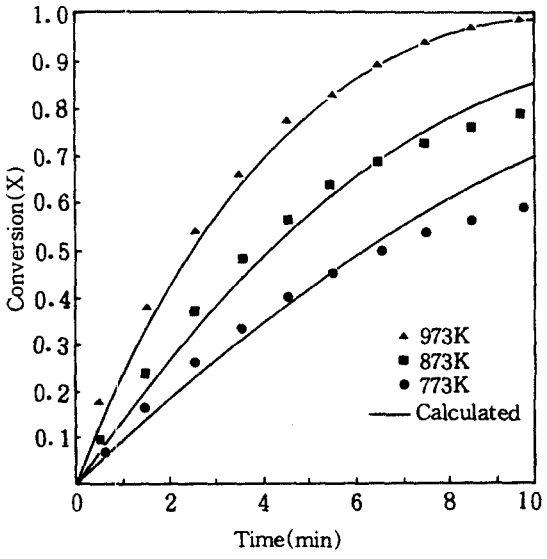


Fig. 16. Comparison between experimental data and calculated data for the sorbents (ZnO-10 at. % $Fe_2O_3$).

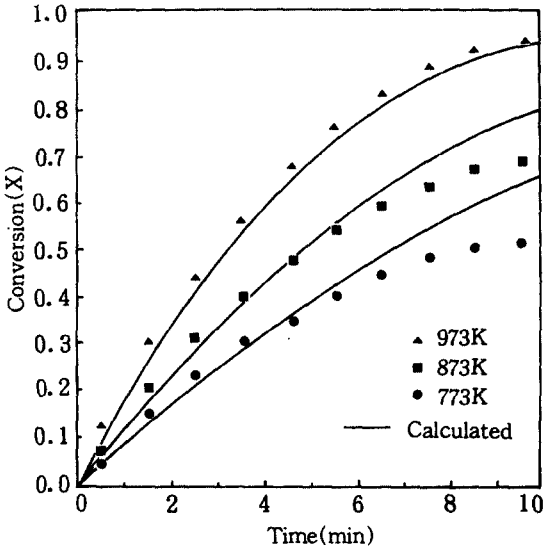


Fig. 17. Comparison between experimental data and calculated data for the sorbents (ZnO-20 at. % $Fe_2O_3$).

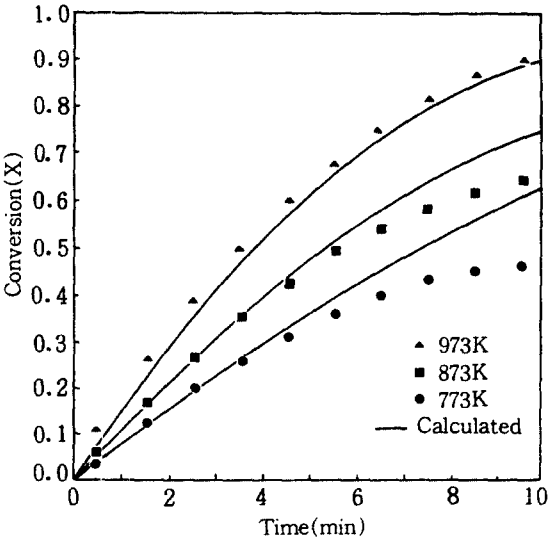


Fig. 18. Comparison between experimental data and calculated data for the sorbents (ZnO-30 at. % $Fe_2O_3$).

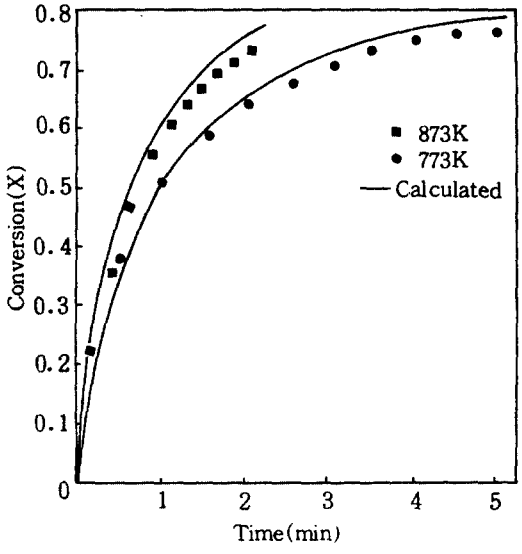


Fig. 19. Comparison between experimental data and calculated data for the sorbents (ZnO-2.0 at. % $Fe_2O_3$).

(-3908.37/T) cm/sec

for ZnO−20 at.% $Fe_2O_3$ $k_s = 0.00491\exp$ (-3945.99/T) cm/sec

for ZnO−30 at.% $Fe_2O_3$ $k_s = 0.00436\exp$ (-3953.61/T) cm/sec

for ZnO−40 at.% $Fe_2O_3$ $k_s = 0.00377\exp$ (-3977.77/T) cm/sec

for ZnO−50 at.% $Fe_2O_3$ $k_s = 0.00415\exp$ (-4216.07/T) cm/sec

And Table 4 list the activation energy E obtained from previous Arrehenius plot. The values of Ea are about 7.8~8.4 kcal. Reflecting the mono-dispersed layer on the platinum cell and high porosity of sorbent, this lower values are considered to be suitable.

### 4. Comparison of Experimental Data with Model

To check the suitability of model, experimental conversion X and theoretical conversion $X_{cal}$ are compared. In terms of conversion X, Eq. (13) becomes

$$X_{cal} = 1-(1-t/t_1)^{2/3} \quad \cdots\cdots (14)$$

At arbitary time t, $X_{cal}$ versus t curve obtained from the substitution of time parameter into Eq.(14) is compared with the experimental conversion vs. time curve. Fig. 16~19 are the typical curves of comparison for sorbents containing 10, 20, 30 and 2 at% $Fe_2O_3$. While the coincidence of experimental and theoretical curves is confirmed over all reaction time at 973K, at low conversion they coincide asymtotcally and at high conversion there are 10~20% deviation between them.

From the sequential studies on additives like $Li_2O$, CaO, and $TiO_2$, we find out pore blocking model shows good aggrement of experimental and theoretical values over all the reaction time, although, it exhibits large deviation between them for sulfidation of pellet-type sorbents. This feature is considered to be caused by pore diffusion between core of pellet and surface and film resistance between bulk stream and pellet surface. So we adopt the grain model

## Ⅳ. Results and Discussions of Adsorption Efficiency

From the previous results, as ZnO-10 at.% $Fe_2O_3$ has similar reaction rate with that of ZnO and high mechanical strength, the experiments for adsorption efficiency were carried out for ZnO-10 at% $Fe_2O_3$ sorbent only.

Fig. 20 shows the concentration of $H_2S$ within outlet gases during sulfidation of which inlet gas flow rate is 200cc/min ($H_2S$ = 2 vol%, $N_2$ = 98 vol%) at 973 K where t is reaction time, t* is time desired to completely change of ZnO to ZnS(20 min), C-O is fresh sorbent, C-1 is lst sulfidation-regeneration cycle sorbent, and C-2 is 2nd sulfidation-regeneration cycle sorbent.

Below $t/t^* = 0.1$, there's no $H_2S$ gas within

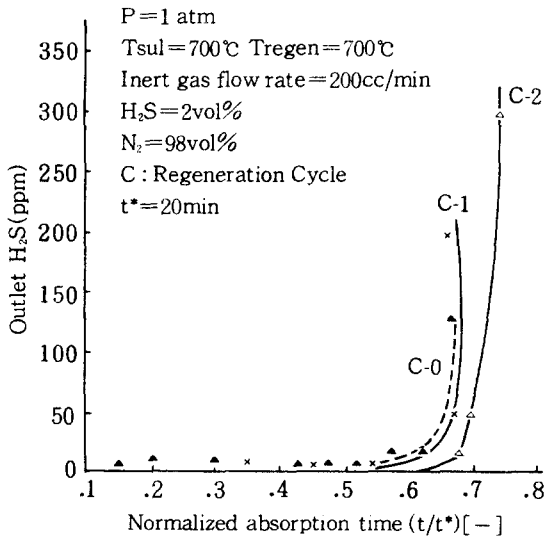


Fig. 20. Breakthrough curves in successive sulfidation cycles of zinc ferrite sorbent (ZnO-10 at. % $Fe_2O_3$) at 700℃.

outlet gases and outlet gases contain $H_2S$ gas below 10ppm for $t/t^* = 0.1 \sim 0.6$, that is, $H_2S$ gas contained initial coal-derived gas is almost removed. As regenerated sorbent (c-1 and c-2) have higher adsorption efficiency than that of fresh sorbent, regenerated sorbent will be used repeatedly by redox method. Thus ZnO-10 at. % $Fe_2O_3$ sorbent is considered to be suitable for $H_2S$ removal.

## V. Conclusions

From the kinetic studies of zinc ferrite with $H_2S$ analyzed by thermogravimetric method, we conclude as follows ;

1) Grain model assuming the controlling step of zinc ferrite sulfidation is chemical reaction is used at high temperature (above 700℃) and low conversion.

2) Sulfidation of zinc ferrite is first order with respect to $H_2S$ concentration.

3) From the viewpoint of kinetics, ZnO containing $Fe_2O_3$ below 2.0 at.% has higher reaction rate than that of pure ZnO and for ZnO-10 at.% $Fe_2O_3$, its reaction rate is similar with ZnO. Above 10. at.% $Fe_2O_3$, reaction rate is decreased, however, mechanical strength is enhanced.

4) From the viewpoint of economics, ZnO-10 at.% $Fe_2O_3$ possessing similar adsorption efficiency with ZnO and high mechanical strength is pratical and suitable for $H_2S$ removal.

### 1) Acknowledgement

We give great thanks to Korea Science and Engineering Foundation with sincere financial assistance.

## Reference

1) Bureau, A.C., and M.J.F. Olden., Chem. Eng. Sci., **49**, 55, 1967.
2) Phillipson, J.J., "Desulfurization in Catalyst Handbook", Wolf, London, England, 1970.
3) Tamhankar S.S. and C.Y. Wen ACS Symposium Series, **223**, 225 1983.
4) Westmoreland Phillip R., James B. Gibson, and Douglas P. Harrison. Envir. Sci. Tech. **11**(5), 488~491, 1985.
5) Anderson G.L., P.C. Garrgan and F.O. Berry, Proc-Electronchem. Soc. 1984, 84~13(Molten Carbonate Fuel Cell) 297~330, (ENG) 1984.
6) Won S. and H.Y. Sohn, Metal. Trans. B **16**B, 163~168, 1985.
7) Krishnan G.N., R.H. Lamoreaux, R.D. Brittain and B.J. Woo. "Investigation of Sulfate Formation During Regeneration of Zinc Ferrite Sorbent", Quartery Technical Process Report I, DOE/DE-AC 21~83 MC 20092, SRI Project No. DYU 6433, 1983.
8) Tamhanker S.S., M. Hasatani and C.Y. Wen Chem. Eng. Sci. **36**, 1181, 1981.
9) Gavalas G.R., S.S Tamhanker, M. Bagaiewicz, P.K. Sharma and M.F. Stephanopoulos, Ind. Eng. Chem. Process. Des. Dev., **25**, 429~437, 1986.
10) Thomas Grindley and George Seinfield, U. S. Department of Energy Technical Center, DOE/MC/16545~1125(DE82011114), 1983.
11) Lee, J.B., K.O. Yoo., Korean Journal of Environmental Health Society., **14**, 11, 1988.
12) Seo, I.S. J.B. Lee, K.O. Yoo., Korean Journal of Environmental Health Society., **14**, 1, 1988.
13) Won, H., master thesis, Hanyang University 1988. 2